



# Rapid calibration method for measuring linear axis optical paths of computer numerical control machine tools with a laser interferometer

Xiaogeng Jiang<sup>1,2</sup> · Tianfang Meng<sup>1,2</sup> · Liang Wang<sup>1,2</sup> · Chang Liu<sup>1,2</sup>

Received: 17 February 2020 / Accepted: 17 August 2020 / Published online: 22 September 2020  
© Springer-Verlag London Ltd., part of Springer Nature 2020

## Abstract

The optical path calibration process using a laser interferometer is time-consuming and tedious, requiring repeated adjustment and experienced operators, leading to a significant reduction in measuring efficiency. A novel optical path calibration process of the linear axis of a three-axis machine tool using a Renishaw XL-80 laser interferometer is proposed in this paper. The homogeneous coordinate transformation error model of the measured axis is established. Using the established error model, only the initial distance from the laser transmitter to the beam splitter and the initial distance from the beam splitter to the linear mirror are required to accurately calibrate the laser beam. The relationship between the fixed distance from the center of the light target to the quarter point on the edge of the light target and the movement distance of the measured axis are obtained. Eight deviations of the optical path affected by the laser transmitter, the beam splitter and the linear mirror are solved. Calibrations based on the deviations can be achieved by adjusting the positions and orientations of the laser interferometer components, leading to a rapid and accurate calibration method for measuring the optical paths.

**Keywords** Laser interferometer · CNC machine tool · Error model · Optical path calibration

## 1 Introduction

Laser interferometry has been used extensively in the precision inspection field such as error measurement and instrument calibration [1–6]. Dual-frequency laser interferometers are a major type of laser interferometry application, which are widely used in error measurement and compensation of multi-axis machine tools and coordinate measuring machines [7–9]. In order to reduce the Abbe error between the optical path and the measured motion axis during the setup process of the laser interferometer system, as well as the cosine error caused by the multi-degree of freedom motion of the measured axis during measurement [10], the optical path of the laser interferometer should therefore be calibrated and adjusted accordingly. However, the optical path calibration and adjustment of the

laser interferometer is time-consuming and require experienced operators [11–13].

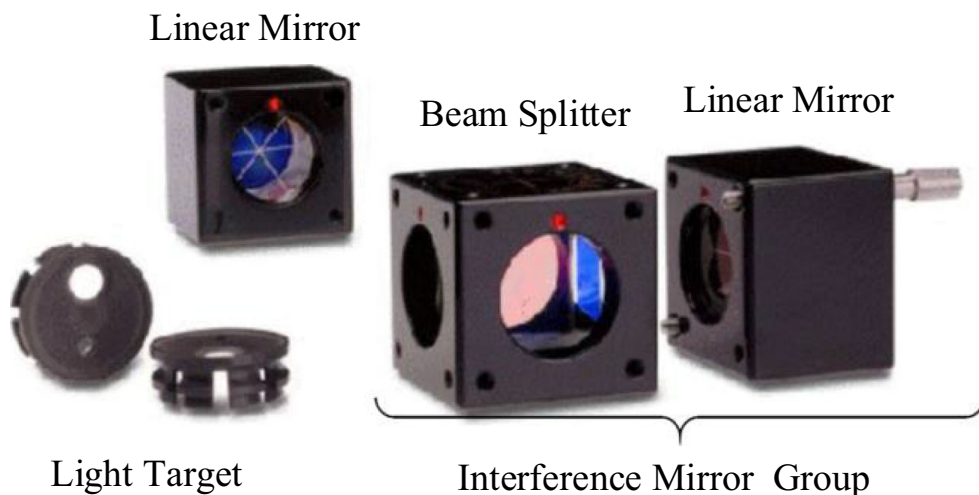
At present, several adjustment methods are available for optical calibration process. Chen introduced a triangle adjustment method to measure the positioning errors of a machine tool by replacing the magnetic base with a gauge block frame and a pentagonal prism to reduce the measurement error [14]. Zhang et al. developed a laser interferometer automatic aiming system for the spatial error measurement of CNC machine tools. They also proposed a direct measurement to obtain the entire spatial positioning error of CNC machine tools through a pair of light beams [15]. Wei set up an outline of a detailed operation process of the adjustment method using a laser interferometer [16]. In order to quickly and accurately adjust the laser direction, Liu et al. analyzed the causes of laser beam eccentricity and designed a control unit to adjust the translation and rotation motion of the interferometer to achieve the laser interferometer beam collimation [17]. Shi proposed a fast and accurate adjustment method of a laser interferometer according to a proportional method [18]. On the basis of fully analyzing the principle of the optical path adjustment, Wu et al. designed and manufactured a specific platform for the vertical axis and used it in practice for the purpose of

✉ Chang Liu  
liuchang@tiangong.edu.cn

<sup>1</sup> Tianjin Key Laboratory of Advanced Mechatronics Equipment Technology, Tiangong University, Tianjin 300387, China

<sup>2</sup> School of Mechanical Engineering, Tiangong University, Tianjin 300387, China

Fig. 1 Optical mirrors



calibration [19]. Gong et al. established a mathematical model of the optical path of the laser interferometer in the spatial coordinate system, and compensated for the efficiency loss caused by the operator’s lack of experience by analyzing the influence of different regulators on the optical path [20].

The idea of the current calibration processes is to repeatedly adjust the laser interferometer components after rough adjustment on the machine tool, resulting in low efficiency and time-consuming process. No quantitative indication can be given for the adjustment, thus the adjusting process is highly dependent upon the experience of the operator, which makes the adjustment not accurate enough for testing. Therefore, this article is aiming at a guideline for operators with less operation skill to adjust the optical path within shorter period but better accuracy. In this paper, the quantitative adjustment amount of the laser interferometer components can be obtained with the homogeneous transformation matrix (HTM) modeling the laser beam. A Renishaw XL-80 laser interferometer is used to calibrate

the X-, Y-, and Z-axes of two Hanchuan XK714D CNC milling machines for validation purposes.

The remainder of this paper is organized as follows. Section 2 introduces the laser interferometer measuring system. Section 3 gives the optical path error model using the HTMs. In the fourth section, the experiment process is described and the errors of each component are obtained. The fifth part presents the optical path adjustment according to the errors obtained in Section 4. The last section gives the conclusions.

## 2 Laser interferometer system

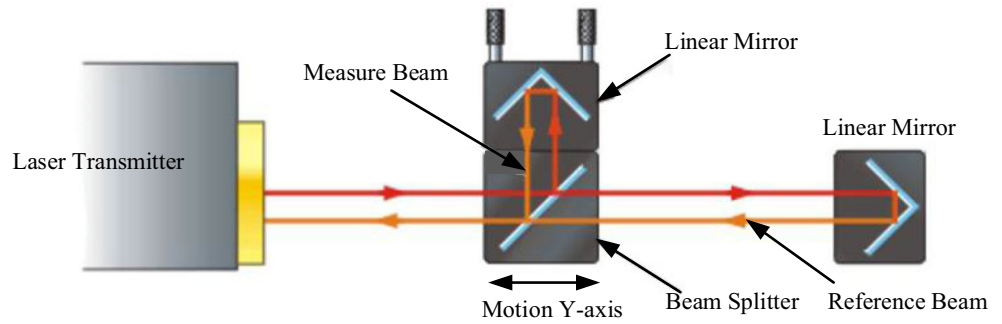
### 2.1 Equipment

The laser interferometer system includes two light targets, a beam splitter, two linear mirrors, an interference mirror group (made up by a linear mirror with a beam splitter), an XL-80

Fig. 2 The Renishaw XL-80 measuring equipment



**Fig. 3** The principle of detecting the X- and Y-axes



laser transmitter, a universal tripod, a Renishaw XL-80 environmental compensation unit, a temperature sensor, and an air temperature sensor, as shown in Figs. 1 and 2.

**2.2 Principle of the laser interferometer measurement**

The laser emitted from the laser transmitter is dispersed into two coherent beams after passing through the beam splitter, namely, the two reflected lights of different paths. When the optical path of the X-, Y-, and Z-axes are detected, one reflected light will be reflected back to the receiving end of the laser transmitter by the linear mirror, and the other reflected light will be reflected back to the receiving end of the laser transmitter by the fixed linear mirror. The measure beam and reference beam (orange light in Figs. 3 and 4) are superimposed on the interference mirror group, and the two beams are finally detected and compared in the detector at the laser receiver [21, 22], as shown in Figs. 3 and 4.

**3 Optical path error model**

**3.1 Optical path error modeling of the X- and Y-axis detection**

The light beam from the laser transmitter reaches the beam splitter coordinate system  $O_1-X_1Y_1Z_1$  along the Y-axis relative

to the laser transmitter coordinate system  $O_0-X_0Y_0Z_0$ ; the beam transmitted from the beam splitter reaches the coordinate system  $O_2-X_2Y_2Z_2$  of the linear mirror, as shown in Fig. 5. The major component errors affecting the laser beam are shown in Fig. 6 and Table 1. The following mathematical model is established for the detection system.

where the superscript represents the optical path of the Y-axis; the subscript represents the error direction; the translation error is represented by  $\delta$ ; the angle error is represented by  $\epsilon$ ; and the letter in the parentheses represents the component that contains the error. The laser transmitter is represented by  $l$ , the beam splitter is represented by  $s$ , and the linear mirror is represented by  $r$ .

- 1) The laser transmitter point is set as the coordinate origin. Therefore, the laser transmitter is ideally an identity matrix:

$$I_l = I_4 \tag{1}$$

The errors affecting the laser transmitter are mainly caused by the translations along the X- and Z-axes and rotations around the X- and Z-axes. Hence,

$$\Delta T_{Y\delta_x(l)} = \begin{bmatrix} 1 & 0 & 0 & Y\delta_x(l) \\ 0 & 1 & 0 & 0 \\ 0 & 0 & 1 & 0 \\ 0 & 0 & 0 & 1 \end{bmatrix} \tag{2}$$

**Fig. 4** The principle of detecting the Z-axis

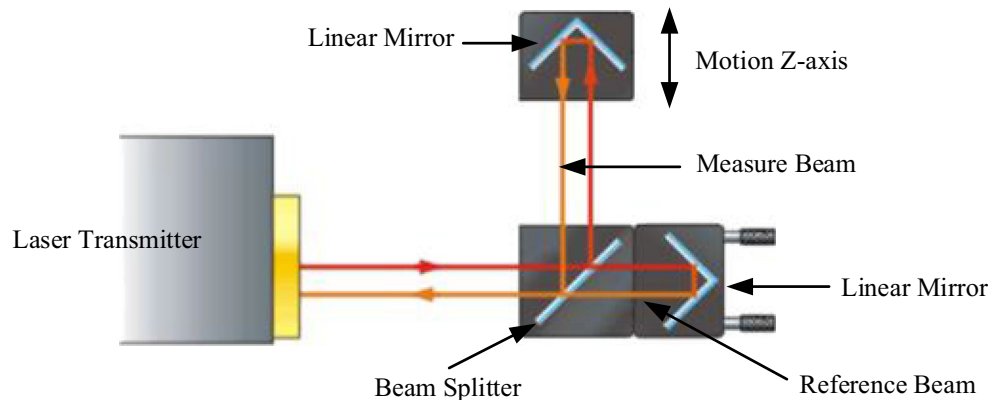
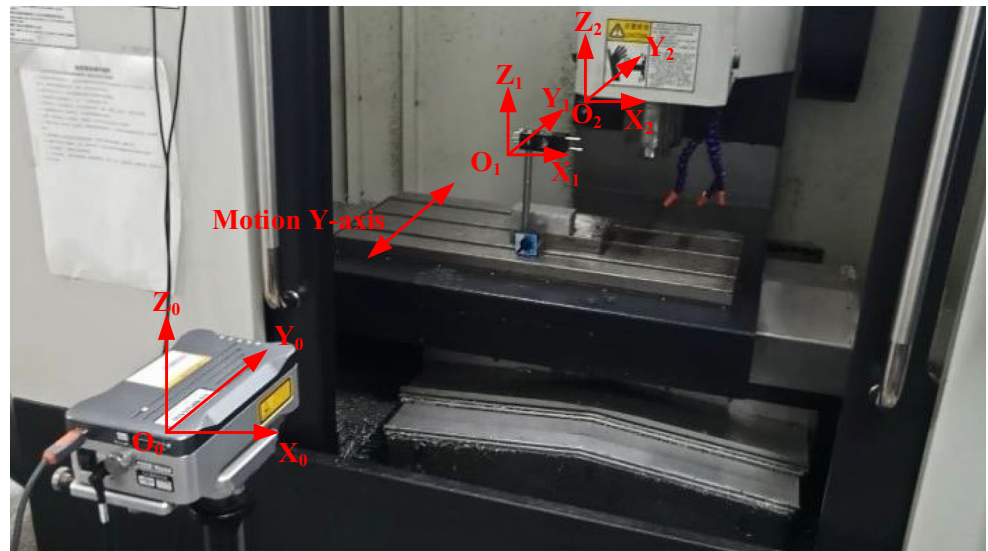


Fig. 5 Schematic view of the X- and Y-axis coordinate assignment



where  $\Delta T_{Y\delta_x(l)}$  is the error transformation matrix of the translation error  ${}^Y\delta_x(l)$  of the laser transmitter in the X-axis direction.

$$\Delta T_{Y\delta_z(l)} = \begin{bmatrix} 1 & 0 & 0 & 0 \\ 0 & 1 & 0 & 0 \\ 0 & 0 & 1 & {}^Y\delta_z(l) \\ 0 & 0 & 0 & 1 \end{bmatrix} \quad (3)$$

where  $\Delta T_{Y\delta_z(l)}$  is the error transformation matrix of the translation error  ${}^Y\delta_z(l)$  of the laser transmitter in the Z-axis direction.

$$\Delta T_{Y\epsilon_x(l)} = \begin{bmatrix} 1 & 0 & 0 & 0 \\ 0 & \cos^Y\epsilon_x(l) & -\sin^Y\epsilon_x(l) & 0 \\ 0 & \sin^Y\epsilon_x(l) & \cos^Y\epsilon_x(l) & 0 \\ 0 & 0 & 0 & 1 \end{bmatrix} \quad (4)$$

where  $\Delta T_{Y\epsilon_x(l)}$  is the error transformation matrix of the pitch angle  ${}^Y\epsilon_x(l)$  of the laser transmitter around the X-axis.

$$\Delta T_{Y\epsilon_z(l)} = \begin{bmatrix} \cos^Y\epsilon_z(l) & -\sin^Y\epsilon_z(l) & 0 & 0 \\ \sin^Y\epsilon_z(l) & \cos^Y\epsilon_z(l) & 0 & 0 \\ 0 & 0 & 1 & 0 \\ 0 & 0 & 0 & 1 \end{bmatrix} \quad (5)$$

where  $\Delta T_{Y\epsilon_z(l)}$  is the error transformation matrix of the yaw angle  ${}^Y\epsilon_z(l)$  of the laser transmitter around the Z-axis.

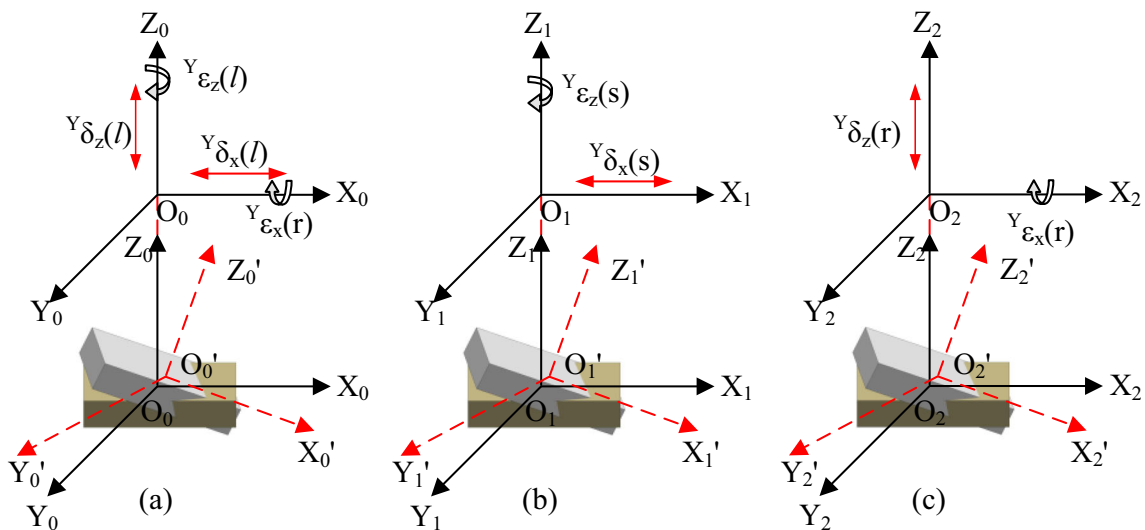


Fig. 6 Component errors of the X- and Y-axes. a Laser transmitter coordinate system. b Beam splitter coordinate system. c Linear mirror coordinate system

Based on Eqs. 1–5, the comprehensive error transformation matrix of the laser transmitter point is given as follows:

$$E_{l1} = \Delta T^Y_{\delta_x(l)} \Delta T^Y_{\delta_z(l)} \Delta T^Y_{\epsilon_x(l)} \Delta T^Y_{\epsilon_z(l)} I_l = \begin{bmatrix} \cos^Y \epsilon_z(l) & -\sin^Y \epsilon_z(l) & 0 & {}^Y \delta_x(l) \\ \cos^Y \epsilon_x(l) \sin^Y \epsilon_z(l) & \cos^Y \epsilon_x(l) \cos^Y \epsilon_z(l) & -\sin^Y \epsilon_x(l) & 0 \\ \sin^Y \epsilon_x(l) \sin^Y \epsilon_z(l) & \cos^Y \epsilon_z(l) \sin^Y \epsilon_x(l) & \cos^Y \epsilon_x(l) & {}^Y \delta_z(l) \\ 0 & 0 & 0 & 1 \end{bmatrix} \quad (6)$$

2) When the laser beam reaches the beam splitter coordinate system  $O_1-X_1Y_1Z_1$ , the ideal matrix is

$$I_{s1} = \begin{bmatrix} 1 & 0 & 0 & 0 \\ 0 & 1 & 0 & Y_s \\ 0 & 0 & 1 & 0 \\ 0 & 0 & 0 & 1 \end{bmatrix} \quad (7)$$

The errors affecting the beam splitter are mainly caused by the translation along the  $X$ -axis of the beam splitter and rotation around the  $Z$ -axis. Hence,

$$\Delta T^Y_{\delta_x(s)} = \begin{bmatrix} 1 & 0 & 0 & {}^Y \delta_x(s) \\ 0 & 1 & 0 & 0 \\ 0 & 0 & 1 & 0 \\ 0 & 0 & 0 & 1 \end{bmatrix} \quad (8)$$

where  $\Delta T^Y_{\delta_x(s)}$  is the error transformation matrix of the translation error  ${}^Y \delta_x(s)$  of the beam splitter in the  $X$ -axis direction.

$$\Delta T^Y_{\epsilon_z(s)} = \begin{bmatrix} \cos^Y \epsilon_z(s) & -\sin^Y \epsilon_z(s) & 0 & 0 \\ \sin^Y \epsilon_z(s) & \cos^Y \epsilon_z(s) & 0 & 0 \\ 0 & 0 & 1 & 0 \\ 0 & 0 & 0 & 1 \end{bmatrix} \quad (9)$$

where  $\Delta T^Y_{\epsilon_z(s)}$  is the error transformation matrix of the yaw angle  ${}^Y \epsilon_z(s)$  of the beam splitter around the  $Z$ -axis.

Therefore, the comprehensive error transformation matrix of the beam splitter is given as follows:

$$E_{s1} = \Delta T^Y_{\delta_x(s)} \Delta T^Y_{\epsilon_z(s)} I_{s1} = \begin{bmatrix} \cos^Y \epsilon_z(s) & -\sin^Y \epsilon_z(s) & 0 & {}^Y \delta_x(s) - Y_s \sin^Y \epsilon_z(s) \\ \sin^Y \epsilon_z(s) & \cos^Y \epsilon_z(s) & 0 & Y_s \cos^Y \epsilon_z(s) \\ 0 & 0 & 1 & 0 \\ 0 & 0 & 0 & 1 \end{bmatrix} \quad (10)$$

3) When the laser beam reaches the coordinate system  $O_2-X_2Y_2Z_2$  of the linear mirror, the ideal matrix is

$$I_{r1} = \begin{bmatrix} 1 & 0 & 0 & 0 \\ 0 & 1 & 0 & Y_r \\ 0 & 0 & 1 & 0 \\ 0 & 0 & 0 & 1 \end{bmatrix} \quad (11)$$

The errors affecting the linear mirror are mainly caused by the translation along the  $Z$ -axis of the linear mirror and rotation around the  $X$ -axis. Hence,

$$\Delta T^Y_{\delta_z(r)} = \begin{bmatrix} 1 & 0 & 0 & 0 \\ 0 & 1 & 0 & 0 \\ 0 & 0 & 1 & {}^Y \delta_z(r) \\ 0 & 0 & 0 & 1 \end{bmatrix} \quad (12)$$

where  $\Delta T^Y_{\delta_z(r)}$  is the error transformation matrix of the translation error  ${}^Y \delta_z(r)$  of the linear mirror in the  $X$ -axis direction.

$$\Delta T^Y_{\epsilon_x(r)} = \begin{bmatrix} 1 & 0 & 0 & 0 \\ 0 & \cos^Y \epsilon_x(r) & -\sin^Y \epsilon_x(r) & 0 \\ 0 & \sin^Y \epsilon_x(r) & \cos^Y \epsilon_x(r) & 0 \\ 0 & 0 & 0 & 1 \end{bmatrix} \quad (13)$$

where  $\Delta T^Y_{\varepsilon_x(r)}$  is the error transformation matrix of the pitch angle  ${}^Y\varepsilon_x(r)$  of the linear mirror around the  $X$ -axis.

Therefore, the comprehensive error transformation matrix of the linear mirror is given as follows:

$$E_{r1} = \Delta T^Y_{\delta_z(r)} \Delta T^Y_{\varepsilon_x(r)} I_{r1} = \begin{bmatrix} 1 & 0 & 0 & 0 \\ 0 & \cos^Y\varepsilon_x(r) & -\sin^Y\varepsilon_x(r) & Y_r \cos^Y\varepsilon_x(r) \\ 0 & \sin^Y\varepsilon_x(r) & \cos^Y\varepsilon_x(r) & {}^Y\delta_z(r) + Y_r \sin^Y\varepsilon_x(r) \\ 0 & 0 & 0 & 1 \end{bmatrix} \quad (14)$$

4) The coordinates of the light spot at the beam splitter are given as follows:

$$M_1 = E_{l1} E_{s1} T = \begin{bmatrix} {}^Y\delta_x(l) - Y_s(\cos^Y\varepsilon_z(l)\sin^Y\varepsilon_z(s) + \sin^Y\varepsilon_z(l)\cos^Y\varepsilon_z(s)) + {}^Y\delta_x(s)\cos^Y\varepsilon_z(l) \\ Y_s(\cos^Y\varepsilon_x(l)\cos^Y\varepsilon_z(l)\cos^Y\varepsilon_z(s) - \cos^Y\varepsilon_x(l)\sin^Y\varepsilon_z(l)\sin^Y\varepsilon_z(s)) + {}^Y\delta_x(s)\cos^Y\varepsilon_x(l)\sin^Y\varepsilon_z(l) \\ {}^Y\delta_z(l) + Y_s(\cos^Y\varepsilon_z(l)\sin^Y\varepsilon_x(l)\cos^Y\varepsilon_z(s) - \sin^Y\varepsilon_x(l)\sin^Y\varepsilon_z(l)\sin^Y\varepsilon_z(s)) + {}^Y\delta_x(s)\sin^Y\varepsilon_x(l)\sin^Y\varepsilon_z(l) \\ 1 \end{bmatrix} \quad (15)$$

where  $T = [0 \ 0 \ 0 \ 1]^T$ .

5) The coordinates of the light spot at the linear mirror are given as follows:

$$M_2 = E_{l1} E_{r1} T = \begin{bmatrix} {}^Y\delta_x(l) - Y_r \sin^Y\varepsilon_z(l) \cos^Y\varepsilon_x(r) \\ -Y_r(\sin^Y\varepsilon_x(l)\sin^Y\varepsilon_x(r) - \cos^Y\varepsilon_x(l)\cos^Y\varepsilon_z(l)\cos^Y\varepsilon_x(r)) - {}^Y\delta_z(r)\sin^Y\varepsilon_x(l) \\ {}^Y\delta_z(l) + Y_r(\cos^Y\varepsilon_x(l)\sin^Y\varepsilon_x(r) + \cos^Y\varepsilon_z(l)\sin^Y\varepsilon_x(l)\cos^Y\varepsilon_x(r)) + {}^Y\delta_z(r)\cos^Y\varepsilon_x(l) \\ 1 \end{bmatrix} \quad (16)$$

Since the coordinates of  $M_1$  and  $M_2$  are the same in the  $X$ - and  $Z$ -axis directions. In the  $Y$ -axis direction, there is a  $k_1$  time relationship between the coordinates of  $M_1$  and  $M_2$ , where  $k_1$  represents a value not equal to 1, that is, the values of  $M_1$  and  $M_2$  in the  $Y$ -axis direction are different. According to Eqs. 15 and 16, the relationship between  $M_1$  and  $M_2$  can be obtained as follows:

$$\begin{cases} M_1(1, 1) = M_2(1, 1) \\ M_1(2, 1) = k_1 M_2(2, 1) \\ M_1(3, 1) = M_2(3, 1) \end{cases} \quad (17)$$

### 3.2 Optical path error modeling of the $Z$ -axis detection

The laser beam reaches the beam splitter (coordinate system  $O_1-X_1Y_1Z_1$ ) along the  $Y$ -axis, then passing through the beam

splitter and reaching the linear mirror (coordinate system  $O_2-X_2Y_2Z_2$ ), as shown in Fig. 7. The major component errors affecting the laser beam are shown in Fig. 8 and Table 2. The following mathematical model is established for the detection system.

**Table 1** Main component errors affecting the  $X$ - and  $Y$ -axis optical path

Laser transmitter error	Beam splitter error	Linear mirror error
${}^Y\delta_x(l)$	${}^Y\delta_x(s)$	
${}^Y\delta_z(l)$		${}^Y\delta_z(r)$
${}^Y\varepsilon_x(l)$		${}^Y\varepsilon_x(r)$
${}^Y\varepsilon_z(l)$	${}^Y\varepsilon_z(s)$	

**Fig. 7** Schematic view of the Z-axis coordinate assignment



where the superscript represents the optical path of the Z-axis; the subscript represents the error direction; the translation error is represented by  $\delta$ ; the angle error is represented by  $\varepsilon$ ; and the letter in parentheses represents the component that contain the error. The laser transmitter is represented by  $l$ , the beam splitter is represented by  $s$ , and the linear mirror is represented by  $r$ .

1) The laser transmitter point is set as the coordinate origin. Therefore, the laser transmitter is ideally an identity matrix:

$$I_l = I_4 \tag{18}$$

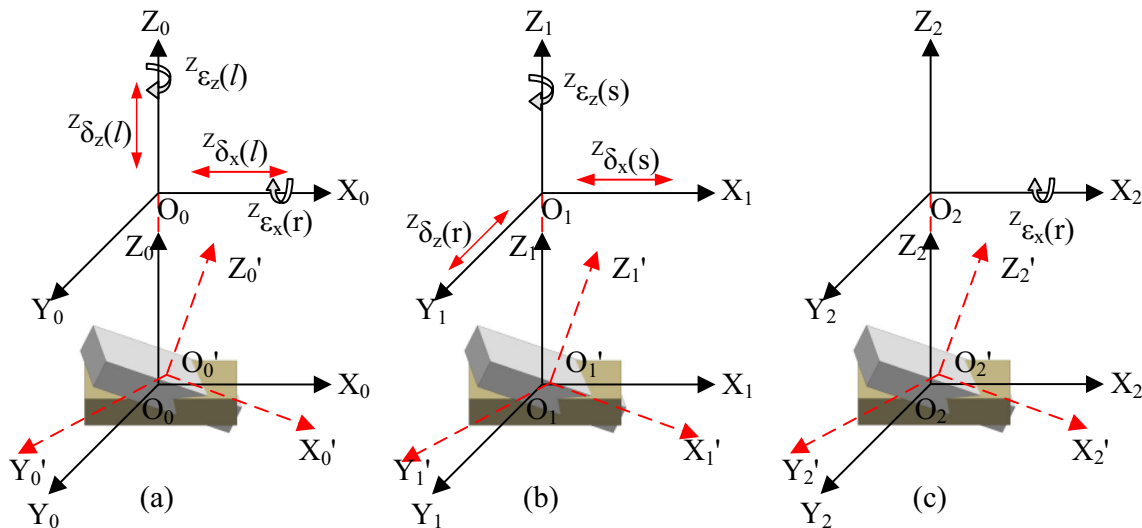


**Fig. 8** Component errors of the Z-axis. **a** Laser transmitter coordinate system. **b** Beam splitter coordinate system. **c** Linear mirror coordinate system

**Table 2** Main component errors affecting the Z-axis optical path

Laser transmitter error	Beam splitter error	Linear mirror error
${}^Z\delta_x(l)$	${}^Z\delta_x(s)$	
	${}^Z\delta_y(s)$	
${}^Z\delta_z(l)$		
${}^Z\varepsilon_x(l)$		${}^Z\varepsilon_x(r)$
${}^Z\varepsilon_z(l)$	${}^Z\varepsilon_z(s)$	

The errors affecting the laser transmitter are mainly caused by the translations along the X- and Z-axes and rotations around the X- and Z-axes. Hence,

$$\Delta T_{Z\delta_x(l)} = \begin{bmatrix} 1 & 0 & 0 & {}^Z\delta_x(l) \\ 0 & 1 & 0 & 0 \\ 0 & 0 & 1 & 0 \\ 0 & 0 & 0 & 1 \end{bmatrix} \tag{19}$$

where  $\Delta T_{Z\delta_x(l)}$  is the error transformation matrix of the translation error  ${}^Z\delta_x(l)$  of the laser transmitter in the X-axis direction.

$$\Delta T_{Z\delta_z(l)} = \begin{bmatrix} 1 & 0 & 0 & 0 \\ 0 & 1 & 0 & 0 \\ 0 & 0 & 1 & {}^Z\delta_z(l) \\ 0 & 0 & 0 & 1 \end{bmatrix} \tag{20}$$

where  $\Delta T_{Z\delta_z(l)}$  is the error transformation matrix of the translation error  ${}^Z\delta_z(l)$  of the laser transmitter in the Z-axis direction.

$$\Delta T_{Z\varepsilon_x(l)} = \begin{bmatrix} 1 & 0 & 0 & 0 \\ 0 & \cos^Z\varepsilon_x(l) & -\sin^Z\varepsilon_x(l) & 0 \\ 0 & \sin^Z\varepsilon_x(l) & \cos^Z\varepsilon_x(l) & 0 \\ 0 & 0 & 0 & 1 \end{bmatrix} \tag{21}$$

where  $\Delta T_{Z\varepsilon_x(l)}$  is the error transformation matrix of the pitch angle  ${}^Z\varepsilon_x(l)$  of the laser transmitter around the X-axis.

$$\Delta T_{Z\varepsilon_z(l)} = \begin{bmatrix} \cos^Z\varepsilon_z(l) & -\sin^Z\varepsilon_z(l) & 0 & 0 \\ \sin^Z\varepsilon_z(l) & \cos^Z\varepsilon_z(l) & 0 & 0 \\ 0 & 0 & 1 & 0 \\ 0 & 0 & 0 & 1 \end{bmatrix} \tag{22}$$

where  $\Delta T_{Z\varepsilon_z(l)}$  is the error transformation matrix of the yaw angle  ${}^Z\varepsilon_z(l)$  of the laser transmitter around the Z-axis.

Based on Eqs. 18–22, the comprehensive error transformation matrix of the laser transmitter point is given as follows:

$$\begin{aligned} E_{l2} &= \Delta T_{Z\delta_x(l)} \Delta T_{Z\delta_z(l)} \Delta T_{Z\varepsilon_x(l)} \Delta T_{Z\varepsilon_z(l)} I_l \\ &= \begin{bmatrix} \cos^Z\varepsilon_z(l) & -\sin^Z\varepsilon_z(l) & 0 & {}^Z\delta_x(l) \\ \cos^Z\varepsilon_x(l)\sin^Z\varepsilon_z(l) & \cos^Z\varepsilon_x(l)\cos^Z\varepsilon_z(l) & -\sin^Z\varepsilon_x(l) & 0 \\ \sin^Z\varepsilon_x(l)\sin^Z\varepsilon_z(l) & \cos^Z\varepsilon_x(l)\sin^Z\varepsilon_z(l) & \cos^Z\varepsilon_x(l) & {}^Z\delta_z(l) \\ 0 & 0 & 0 & 1 \end{bmatrix} \end{aligned} \tag{23}$$

2) When the laser beam reaches the beam splitter coordinate system  $O_1-X_1Y_1Z_1$ , the ideal matrix is

$$I_{s2} = \begin{bmatrix} 1 & 0 & 0 & 0 \\ 0 & 1 & 0 & Z_s \\ 0 & 0 & 1 & 0 \\ 0 & 0 & 0 & 1 \end{bmatrix} \tag{24}$$

The errors affecting the beam splitter are mainly caused by the translation along the X- and Y-axes of the beam splitter and rotation around the Z-axis. Hence,

$$\Delta T_{Z\delta_x(s)} = \begin{bmatrix} 1 & 0 & 0 & {}^Z\delta_x(s) \\ 0 & 1 & 0 & 0 \\ 0 & 0 & 1 & 0 \\ 0 & 0 & 0 & 1 \end{bmatrix} \tag{25}$$

where  $\Delta T_{Z\delta_x(s)}$  is the error transformation matrix of the translation error  ${}^Z\delta_x(s)$  of the beam splitter in the X-axis direction.

$$\Delta T_{Z\delta_y(s)} = \begin{bmatrix} 1 & 0 & 0 & 0 \\ 0 & 1 & 0 & {}^Z\delta_y(s) \\ 0 & 0 & 1 & 0 \\ 0 & 0 & 0 & 1 \end{bmatrix} \tag{26}$$

where  $\Delta T_{Z\delta_y(s)}$  is the error transformation matrix of the translation error  ${}^Z\delta_y(s)$  of the beam splitter in the Y-axis direction.

$$\Delta T_{Y\varepsilon_z(s)} = \begin{bmatrix} \cos^Y\varepsilon_z(s) & -\sin^Y\varepsilon_z(s) & 0 & 0 \\ \sin^Y\varepsilon_z(s) & \cos^Y\varepsilon_z(s) & 0 & 0 \\ 0 & 0 & 1 & 0 \\ 0 & 0 & 0 & 1 \end{bmatrix} \tag{27}$$



where  $\Delta T^Z_{\varepsilon_z}(s)$  is the error transformation matrix of the yaw angle  $^Z\varepsilon_z(s)$  of the beam splitter around the Z-axis.

Therefore, the comprehensive error transformation matrix of the beam splitter is given as follows:

$$E_{s2} = \Delta T_{z\delta_x(s)} \Delta T_{z\delta_y(s)} \Delta T_{z\varepsilon_z(s)} I_{s2} = \begin{bmatrix} \cos^Z\varepsilon_z(s) & -\sin^Z\varepsilon_z(s) & 0 & {}^Z\delta_x(s) - Z_s \sin^Z\varepsilon_z(s) \\ \sin^Z\varepsilon_z(s) & \cos^Z\varepsilon_z(s) & 0 & {}^Z\delta_y(s) + Z_s \cos^Z\varepsilon_z(s) \\ 0 & 0 & 1 & 0 \\ 0 & 0 & 0 & 1 \end{bmatrix} \tag{28}$$

3) When the laser beam reaches the coordinate system  $O_2-X_2Y_2Z_2$  of the linear mirror, the ideal matrix is

$$I_{r2} = \begin{bmatrix} 1 & 0 & 0 & 0 \\ 0 & 1 & 0 & 0 \\ 0 & 0 & 1 & Z_r \\ 0 & 0 & 0 & 1 \end{bmatrix} \tag{29}$$

where  $\Delta T^Z_{\varepsilon_x}(r)$  is the error transformation matrix of the pitch angle  $^Z\varepsilon_x(r)$  of the linear mirror around the X-axis.

Therefore, the comprehensive error transformation matrix of the linear mirror is given as follows:

$$E_{r2} = \Delta T_{z\varepsilon_x(r)} I_{r2} = \begin{bmatrix} 1 & 0 & 0 & 0 \\ 0 & \cos^Z\varepsilon_x(r) & -\sin^Z\varepsilon_x(r) & -Z_r \sin^Z\varepsilon_x(r) \\ 0 & \sin^Z\varepsilon_x(r) & \cos^Z\varepsilon_x(r) & Z_r \cos^Z\varepsilon_x(r) \\ 0 & 0 & 0 & 1 \end{bmatrix} \tag{31}$$

The error affecting the linear mirror is mainly caused by the rotation around the X-axis. Hence,

$$\Delta T_{z\varepsilon_x(r)} = \begin{bmatrix} 1 & 0 & 0 & 0 \\ 0 & \cos^Z\varepsilon_x(r) & -\sin^Z\varepsilon_x(r) & 0 \\ 0 & \sin^Z\varepsilon_x(r) & \cos^Z\varepsilon_x(r) & 0 \\ 0 & 0 & 0 & 1 \end{bmatrix} \tag{30}$$

4) The coordinates of the light spot at the beam splitter are given as follows:

$$N_1 = E_{l2} E_{s2} T = \begin{bmatrix} {}^Z\delta_x(l) + \cos^Z\varepsilon_z(l) ({}^Z\delta_x(s) - Z_s \sin^Z\varepsilon_z(s)) - \sin^Z\varepsilon_z(l) ({}^Z\delta_y(s) + {}^Z\delta_y(s) \cos^Z\varepsilon_z(s)) \\ \cos^Z\varepsilon_x(l) \cos^Z\varepsilon_z(l) ({}^Z\delta_y(s) + Z_s \cos^Z\varepsilon_z(s)) + \cos^Z\varepsilon_x(l) \sin^Z\varepsilon_z(l) ({}^Z\delta_x(s) - Z_s \sin^Z\varepsilon_z(s)) \\ {}^Z\delta_z(l) + \cos^Z\varepsilon_z(l) \sin^Z\varepsilon_x(l) ({}^Z\delta_y(s) + Z_s \cos^Z\varepsilon_z(s)) + \sin^Z\varepsilon_x(l) \sin^Z\varepsilon_z(l) ({}^Z\delta_x(s) - Z_s \sin^Z\varepsilon_z(s)) \\ 1 \end{bmatrix} \tag{32}$$

where  $T = [0 \ 0 \ 0 \ 1]^T$ .

5) The coordinates of the light spot at the linear mirror are given as follows:

$$N_2 = E_{l2} E_{s2} E_{r2} T = \begin{bmatrix} {}^Z\delta_x(l) + \cos^Z\varepsilon_z(l) ({}^Z\delta_x(s) - Z_s \sin^Z\varepsilon_z(s)) - \sin^Z\varepsilon_z(l) ({}^Z\delta_y(s) + Z_s \cos^Z\varepsilon_z(s)) \cos^Z\varepsilon_x(l) \\ + \sin^Z\varepsilon_x(l) \cos^Z\varepsilon_z(l) (\cos^Z\varepsilon_x(r) \cos^Z\varepsilon_z(s) + \sin^Z\varepsilon_x(l) \cos^Z\varepsilon_z(s)) \\ \cos^Z\varepsilon_x(l) \cos^Z\varepsilon_z(l) ({}^Z\delta_y(s) + Z_s \cos^Z\varepsilon_z(s)) - Z_r \sin^Z\varepsilon_x(l) \cos^Z\varepsilon_x(r) + \cos^Z\varepsilon_x(l) \sin^Z\varepsilon_z(l) ({}^Z\delta_x(s) \\ - Z_s \sin^Z\varepsilon_z(s)) - Z_r \sin^Z\varepsilon_x(r) (\cos^Z\varepsilon_x(l) \cos^Z\varepsilon_z(l) \cos^Z\varepsilon_z(s) - \cos^Z\varepsilon_x(l) \sin^Z\varepsilon_z(l) \sin^Z\varepsilon_z(s)) \\ {}^Z\delta_z(l) + Z_r \cos^Z\varepsilon_x(l) \cos^Z\varepsilon_x(r) + \cos^Z\varepsilon_z(l) \sin^Z\varepsilon_x(l) ({}^Z\delta_y(s) + Z_s \cos^Z\varepsilon_z(s)) \\ + \sin^Z\varepsilon_x(l) \sin^Z\varepsilon_z(l) ({}^Z\delta_x(s) - Z_s \sin^Z\varepsilon_z(s)) \\ - Z_r \sin^Z\varepsilon_x(r) (\cos^Z\varepsilon_z(l) \sin^Z\varepsilon_x(l) \cos^Z\varepsilon_z(s) - \sin^Z\varepsilon_x(l) \sin^Z\varepsilon_z(l) \sin^Z\varepsilon_z(s)) \\ 1 \end{bmatrix} \tag{33}$$

Fig. 9 Construction of the Y-axis laser interferometer system

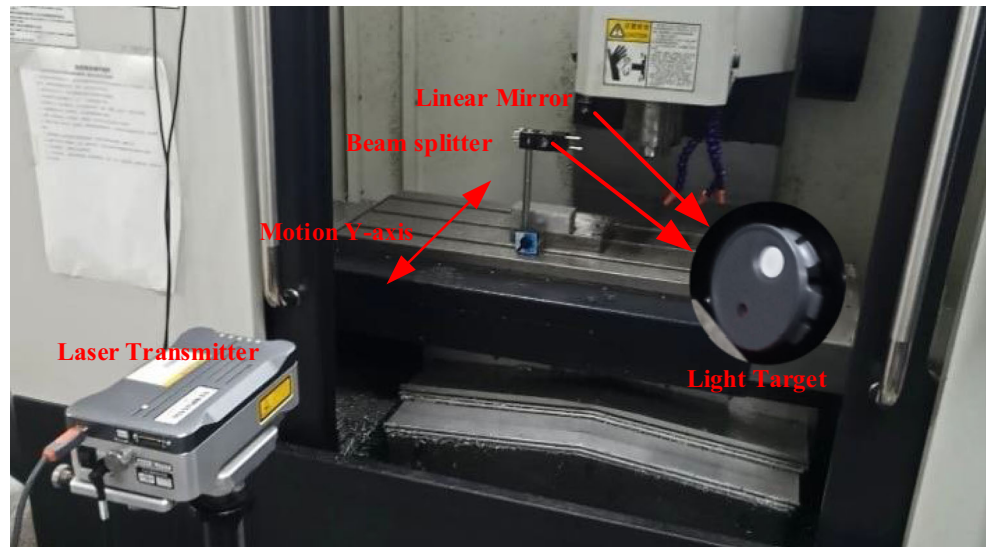


Fig. 10 Schematic diagram of the Y-axis detection optical path

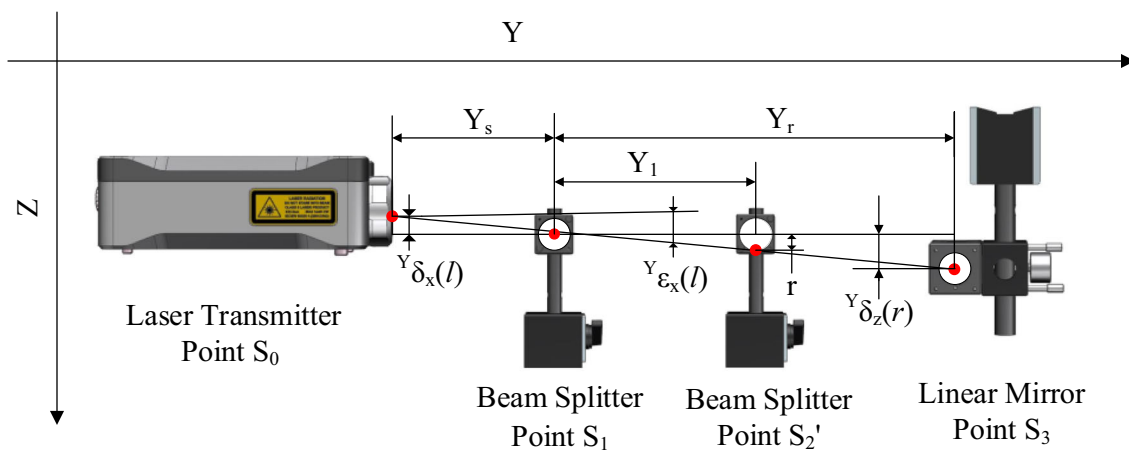
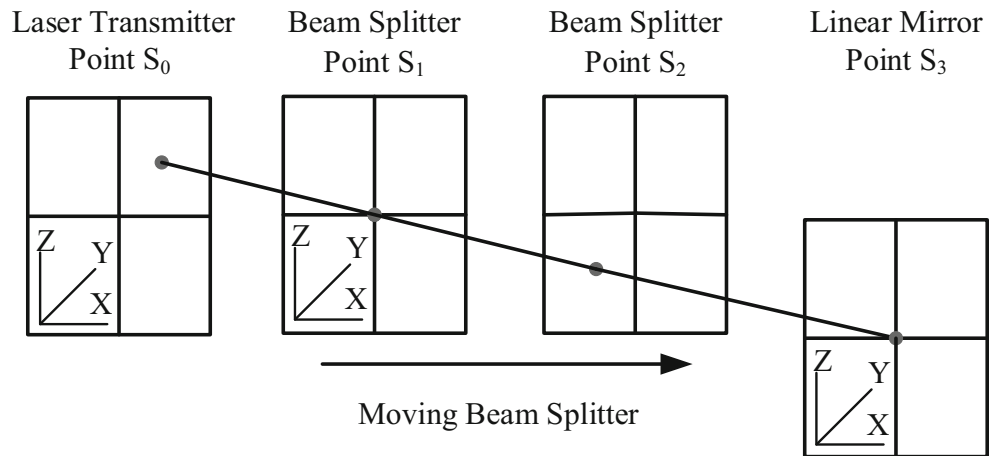
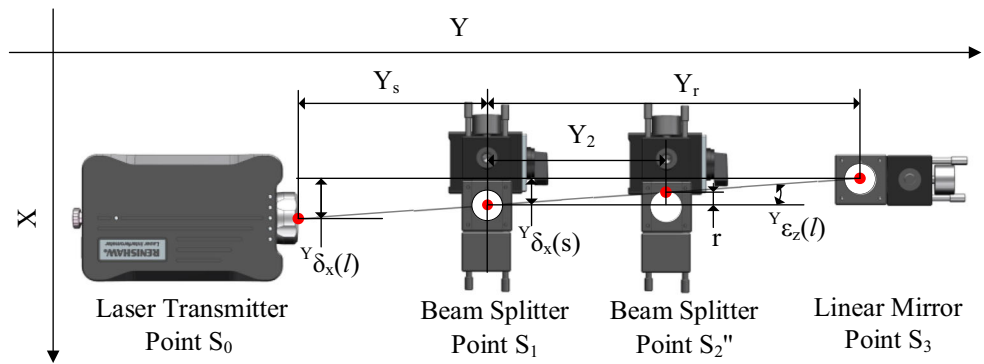


Fig. 11 Laser pitch angle of the Y-axis

Fig. 12 Laser yaw angle of the Y-axis



Since the coordinates of  $N_1$  and  $N_2$  are the same in the X- and Y-axis directions. In the Z-axis direction, there is a  $k_2$  time relationship between the coordinates of  $N_1$  and  $N_2$ , where  $k_2$  represents a value not equal to 1, that is, the values of  $N_1$  and  $N_2$  in the Z-axis direction are different. According to Eqs. 32 and 33, the relationship between  $N_1$  and  $N_2$  can be obtained as follows:

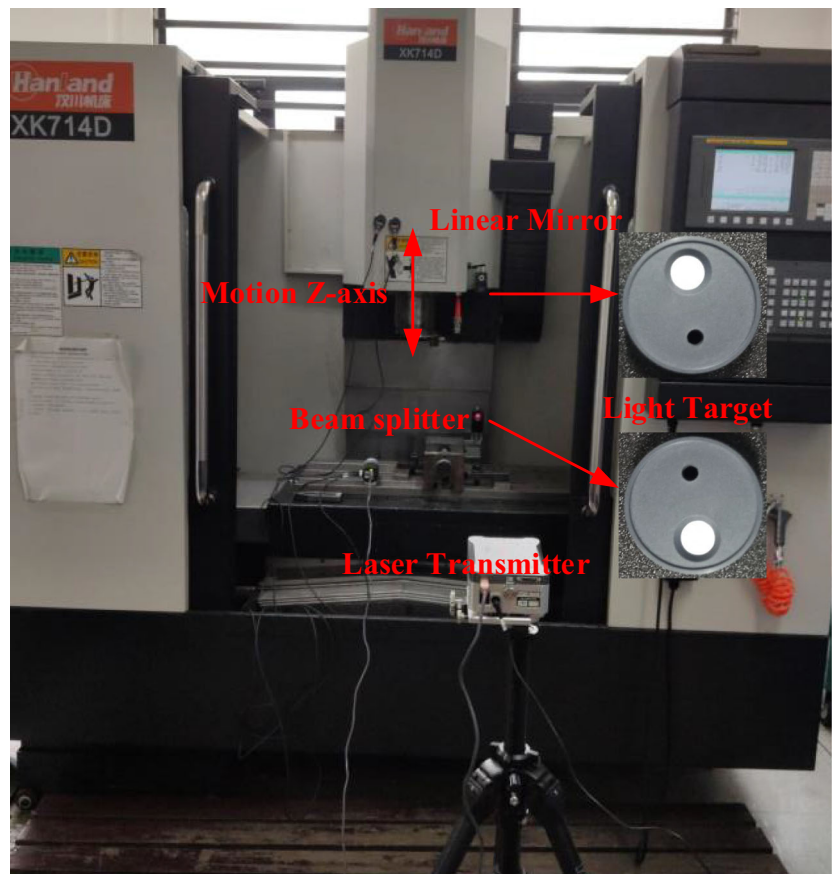
$$\begin{cases} N_1(1, 1) = N_2(1, 1) \\ N_1(2, 1) = N_2(2, 1) \\ N_1(3, 1) = k_2 N_2(3, 1) \end{cases} \quad (34)$$

## 4 Experiment

### 4.1 Measurement of component errors of the horizontal axes

The test bed employed in this paper is a three-axis CNC machine tool manufactured by HanChuan Co., Ltd and the laser interferometer is a Renishaw XL-80. The Renishaw XL-80 laser transmitter is placed on a tripod. The height is adjusted to an appropriate level to the machine bed of the machine tool. The laser interferometer is directly connected to the computer through a USB interface control card. The interferometer

Fig. 13 Construction of the Z-axis laser interferometer system



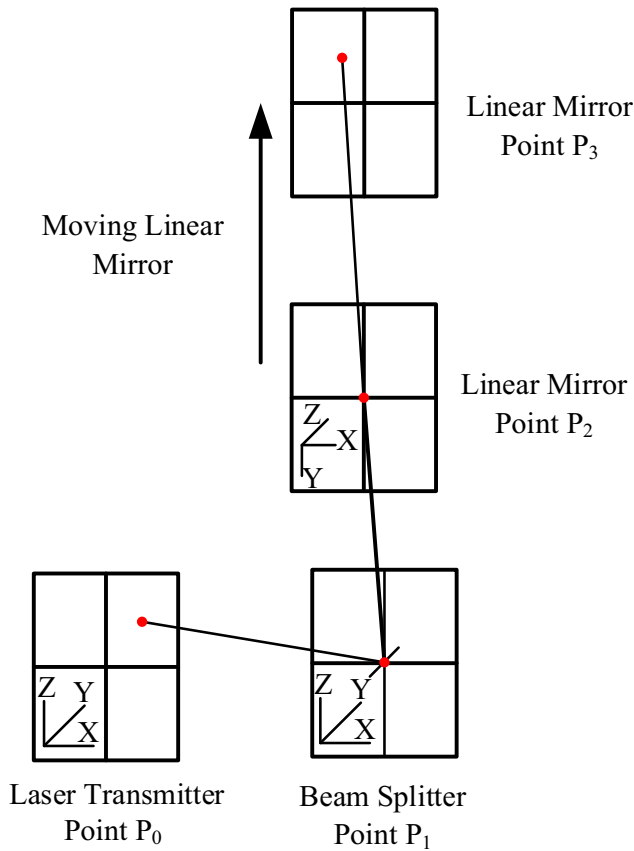


Fig. 14 Schematic diagram of the Z-axis detection optical path

mirror consisting of a beam splitter and a linear mirror is connected to magnetic bases and mounted on the machine table. The other linear mirror is connected to a magnetic base and mounted on spindle housing of the machine tool. The XL-80 environmental compensation unit is attached to the surface of the machine tool table in order to minimize the influence of temperature and air pressure variation. The light targets are mounted on the beam splitter and the linear mirror, where the white spot facing upward, as shown in Fig. 9.

When the Y-axis is moving, the beam splitter point gradually moves from the center to the third quadrant (from  $S_1$  to  $S_2$ ). This implies that the laser beam is actually located in the first quadrant, as shown in Fig. 10. Therefore, the optical path is deviated from its ideal position, and the deviation is to the upper and right side.

First, the Y-axis slide is driven until the beam splitter and the linear mirror are aligned. Then, the Y-axis slide is continuously driven so that the laser beam passes through the center of the beam splitter light target. The distance  $Y_s$  between the laser transmitter point  $S_0$  and the beam splitter point  $S_1$ , and the distance  $Y_r$  between the beam splitter point  $S_1$  and the linear mirror point  $S_3$  are obtained.

Furthermore, the Y-axis slide moves until the beam splitter point  $S_2$  is located at the quarter point of the beam splitter light target, which is denoted as  $S_2'$ . The distance  $Y_1$  (from  $S_1$  to

$S_2'$ ) is obtained, as shown in Fig. 11. The pitch angle  ${}^Y\varepsilon_x(l)$  of the laser transmitter can be calculated based on the moving distance  $Y_1$  and the light target radius  $r$ . Finally, the translation error  ${}^Y\delta_z(l)$  at the laser transmitter and the translation error  ${}^Y\delta_z(r)$  at the linear mirror can be obtained as follows.

$$\begin{cases} \tan({}^Y\varepsilon_x(l)) = \frac{r}{Y_1} \\ Y_s = \frac{{}^Y\delta_z(l)}{\tan({}^Y\varepsilon_x(l))} \\ Y_r = \frac{{}^Y\delta_z(r)}{\tan({}^Y\varepsilon_x(l))} \end{cases} \quad (35)$$

Subsequently, the Y-axis slide moves until the beam splitter point  $S_2$  is located at the quarter point of the beam splitter light target, which is denoted as  $S_2''$ . The distance  $Y_2$  (from  $S_1$  to the  $S_2''$ ) is obtained, as shown in Fig. 12. The yaw angle  ${}^Y\varepsilon_z(l)$  of the laser transmitter can be calculated based on the moving distance  $Y_2$  and the light target radius  $r$ . The translation error  ${}^Y\delta_x(l)$  of the laser transmitter and the translation error  ${}^Y\delta_x(s)$  of the beam splitter can be obtained as follows.

$$\begin{cases} \tan({}^Y\varepsilon_z(l)) = \frac{r}{Y_2} \\ Y_s + Y_r = \frac{{}^Y\delta_x(l)}{\tan({}^Y\varepsilon_z(l))} \\ Y_r = \frac{{}^Y\delta_x(s)}{\tan({}^Y\varepsilon_z(l))} \end{cases} \quad (36)$$

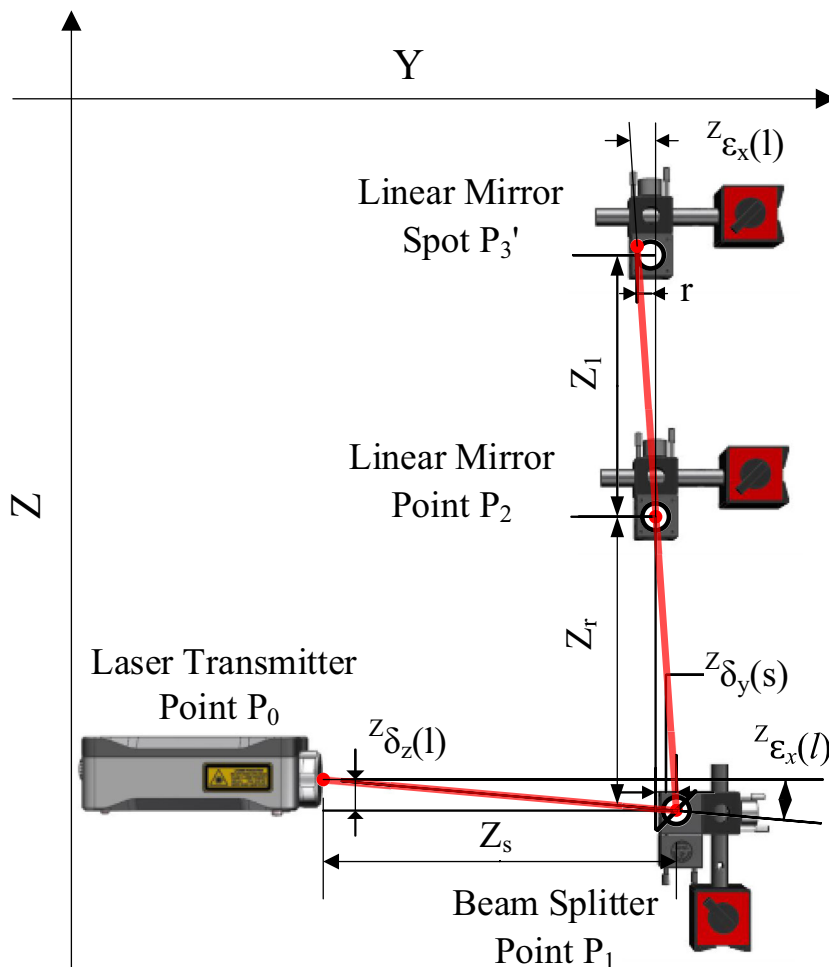
Through the above method, the six unknown variables in the model can be obtained. According to Eq. 17, the yaw angle  ${}^Y\varepsilon_z(s)$  caused by the rotation of the beam splitter around the Z-axis and the pitch angle  ${}^Y\varepsilon_x(r)$  caused by the rotation of the linear mirror around the X-axis can be directly calculated.

### 4.2 Measurement of component errors of the vertical axis

The installation method of the Z-axis experiment is almost the same as that of the Y-axis experiment, apart from the setup of the beam splitter. The interferometer mirror consisting of a beam splitter and a linear mirror is connected to magnetic bases and mounted on the machine table. The other linear mirror is connected to a magnetic base and mounted on spindle housing of the machine tool. The light targets are mounted on the beam splitter and the linear mirror, where the white spot facing downward of the beam splitter and the white spot facing upward of the linear mirror respectively, as shown in Fig. 13.

When the Z-axis is moving, the linear mirror point gradually moves from the center to the second quadrant (from  $P_2$  to  $P_3$ ). This implies that the laser beam is actually located in the first quadrant, as shown in Fig. 14. Therefore, the optical path

Fig. 15 Laser pitch angle of the Z-axis



is deviated from its ideal position, and the deviation is to the upper and right sides.

First, the X- and Y-axis slides are driven until the beam splitter and the linear mirror are aligned. Then, the Z-axis slide is continuously driven so that the laser beam passes through the center of the linear mirror light target. The distance  $Z_s$  between the laser transmitter point  $P_0$  and the beam splitter point  $P_1$ , and the distance  $Z_r$  between the beam splitter point  $P_1$  and the linear mirror point  $P_2$  is obtained.

Furthermore, the Z-axis slide moves until the linear mirror point  $P_3$  is located at the quarter point of the linear mirror light target, which is denoted as  $P_3'$ . The distance  $Z_1$  (from  $P_2$  to  $P_3'$ ) is obtained, as shown in Fig. 15. The pitch angle  ${}^Z\varepsilon_x(l)$  of the laser transmitter can be calculated based on the moving distance  $Z_1$  and the light target radius  $r$ . Finally, the translation error  ${}^Z\delta_z(l)$  at the laser transmitter and the translation error  ${}^Z\delta_y(s)$  at the beam splitter can be as follows:

$$\begin{cases} \tan({}^Z\varepsilon_x(l)) = \frac{r}{Z_1} \\ Z_s = \frac{{}^Z\delta_z(l)}{\tan({}^Z\varepsilon_x(l))} \\ Z_r = \frac{{}^Z\delta_y(s)}{\tan({}^Z\varepsilon_x(l))} \end{cases} \quad (37)$$

Subsequently, the Z-axis slide moves until the linear mirror point  $P_3$  is located at the quarter point of the beam splitter light target, which is denoted as  $P_3''$ . The distance  $Z_2$  (from  $P_2$  to  $P_3''$ ) is obtained, as shown in Fig. 16. The yaw angle  ${}^Z\varepsilon_z(l)$  of the laser transmitter can be calculated based on the moving distance  $Z_2$  and the light target radius  $r$ . The translation error  ${}^Z\delta_x(l)$  at the laser transmitter and the translation error  ${}^Z\delta_x(s)$  at the beam splitter can be obtained as follows:

$$\begin{cases} \tan({}^Z\varepsilon_z(l)) = \frac{r}{Z_2} \\ Z_s = \frac{{}^Z\delta_x(l)}{\tan({}^Z\varepsilon_z(l))} \\ Z_r = \frac{{}^Z\delta_x(s)}{\tan({}^Z\varepsilon_z(l))} \end{cases} \quad (38)$$

Through the above method, the six unknown variables in the model can be obtained. According to Eq. 34, the yaw angle  ${}^Z\varepsilon_z(s)$  caused by the rotation of the beam splitter around the Z-axis and the yaw angle  ${}^Z\varepsilon_x(r)$  caused by the rotation of the linear mirror around the X-axis can be directly calculated.

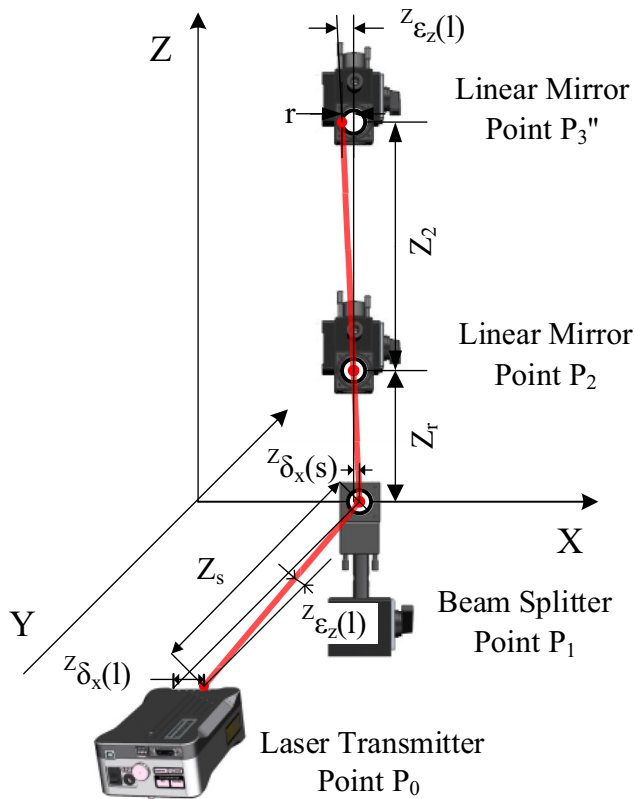


Fig. 16 Laser yaw angle of the Z-axis

In this paper, MATLAB is used to solve the eight deviations of the laser transmitter, the beam splitter, and the linear mirror. The program flow diagram is shown in Fig. 17. The component errors that mainly affect the optical path are shown in Fig. 18 and Table 3.

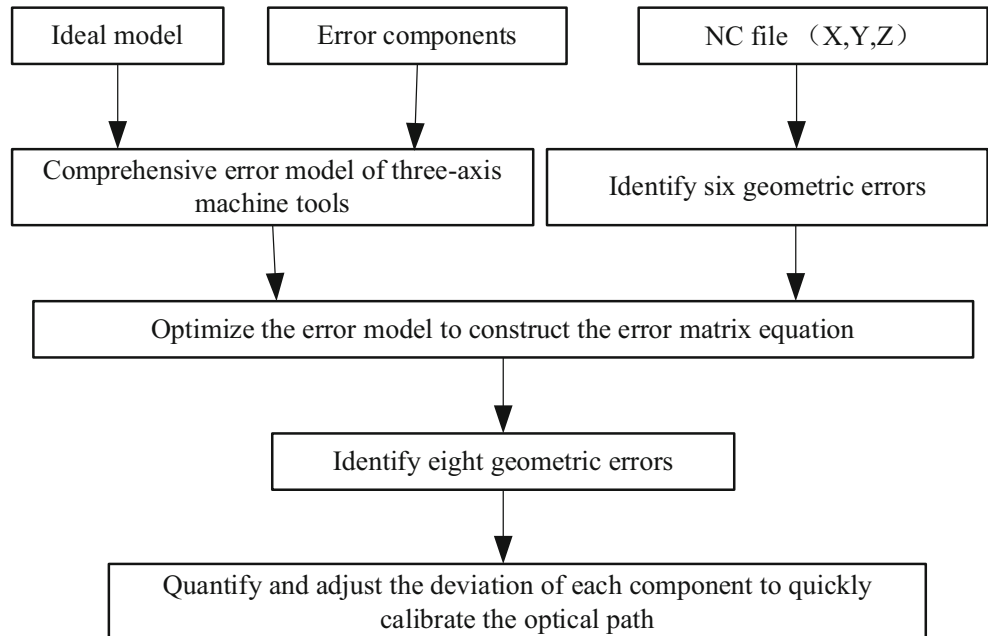
### 5 Adjustment method

#### 5.1 Adjustment method for detecting the horizontal axes optical path

- 1) Adjustment of the upper optical path to the center.

Figure 19 depicts the adjustment process of the upper optical path of the Y-axis to the center. First, the laser transmitter pitch angle knob is adjusted according to the laser pitch angle  $^Y\varepsilon_x(l)$  to cancel it, as shown in Fig. 19b. Then, according to the deviation  $^Y\delta_z(l)$ , the laser transmitter is moved downward so that the beam splitter point  $S_1$  is at the center of the beam splitter light target. Finally, according to the deviation  $^Y\delta_z(r)$ , the linear mirror is moved upward so that the linear mirror point  $S_3$  is at the center of the linear mirror light target, as shown in Fig. 19c. It should be noted that when the laser transmitter point  $S_0$  is located below its ideal position, the adjustment steps are all the same expect that the adjustment direction is opposite.

Fig. 17 Program flow diagram



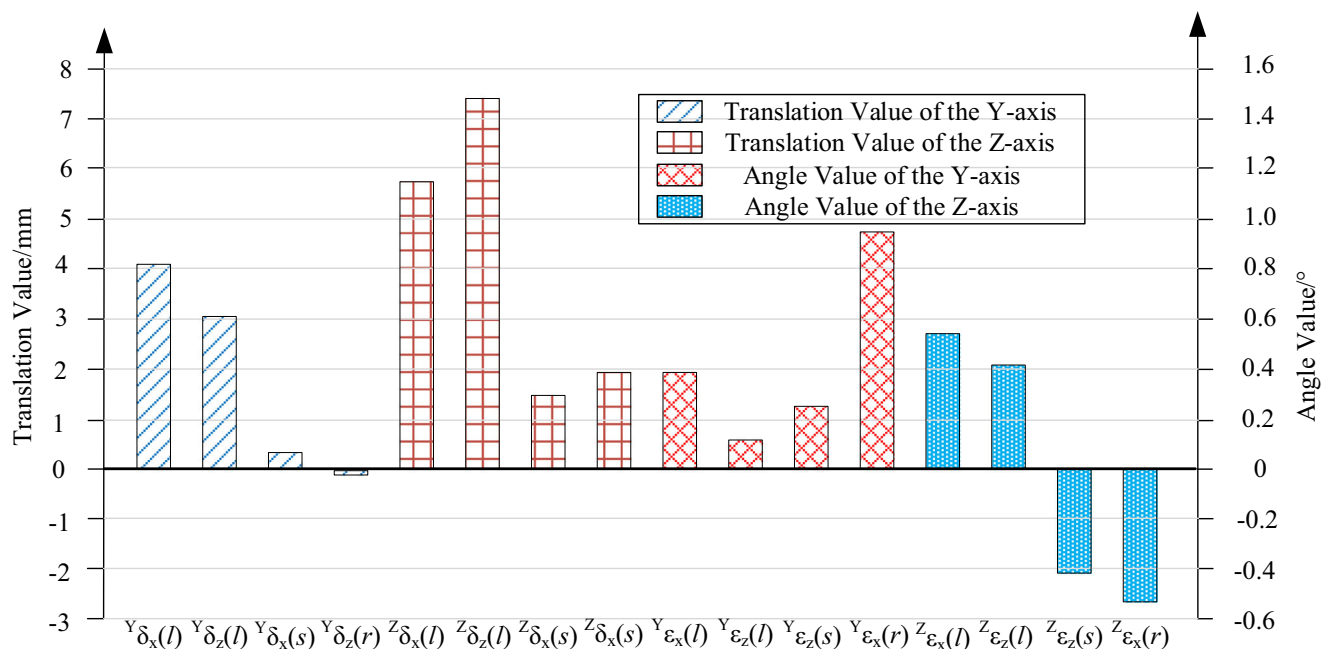


Fig. 18 Component errors of the machine tool affecting the Y- and Z-axis optical path

- 2) Adjustment of the right side optical path to the center.

Figure 20 depicts the adjustment process of the right side optical path of the Y-axis to the center. First, the laser transmitter yaw angle knob is adjusted according to the laser yaw angle  ${}^Y\varepsilon_z(l)$  to cancel it, as shown in Fig. 20b. Then, the laser transmitter is moved left based on the deviation  ${}^Y\delta_x(l)$  and the beam splitter is moved left based on the deviation  ${}^Y\delta_x(s)$ , respectively. Finally, the beam splitter point  $S_1$  and the linear mirror point  $S_3$  are at the center of the light target, as shown in Fig. 20c. It should be noted that when the laser transmitter  $S_0$  is located on the left side of its ideal position, the adjustment steps are all the same except that the adjustment direction is opposite.

Table 3 Major factors affecting the component errors of the optical path of the Y- and Z-axes

Y-axis factors	Y-axis error value	Z-axis factors	Z-axis error value
${}^Y\delta_x(l)$	4.0367 mm	${}^Z\delta_x(l)$	5.8090 mm
${}^Y\delta_z(l)$	3.0049 mm	${}^Z\delta_z(l)$	7.5050 mm
${}^Y\varepsilon_x(l)$	0.0943°	${}^Z\varepsilon_x(l)$	0.5362°
${}^Y\varepsilon_z(l)$	0.1169°	${}^Z\varepsilon_z(l)$	0.4160°
${}^Y\delta_x(s)$	0.3102 mm	${}^Z\delta_x(s)$	1.4523 mm
${}^Y\delta_z(r)$	- 0.0975 mm	${}^Z\delta_y(s)$	1.9420 mm
${}^Y\varepsilon_z(s)$	0.2501°	${}^Z\varepsilon_z(s)$	- 0.4160°
${}^Y\varepsilon_x(r)$	0.9442°	${}^Z\varepsilon_x(r)$	- 0.5362°

### 5.2 Adjustment method for detecting the vertical axis optical path

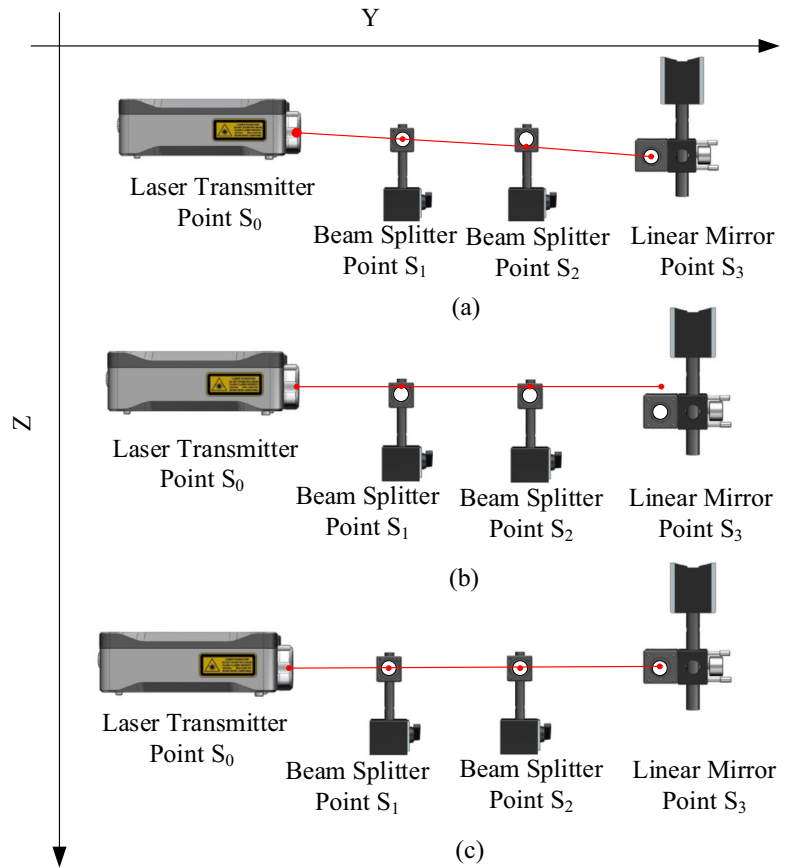
1. Adjustment of the upper optical path to the center.

Figure 21 depicts the adjustment process of the upper optical path of the Z-axis to the center. First, the laser transmitter pitch angle knob is adjusted according to the laser pitch angle  ${}^Z\varepsilon_x(l)$  to cancel it, as shown in Fig. 21b. Then, according to the deviation  ${}^Z\delta_z(l)$ , the laser transmitter is moved downward so that the beam splitter point  $P_1$  is at the center of the beam splitter light target. Finally, according to the deviation  ${}^Z\delta_y(s)$ , the beam splitter is moved forward so that the linear mirror point  $P_2$  is at the center of the linear mirror light target, as shown in Fig. 21c. It should be noted that when the laser transmitter point  $P_0$  is located below its ideal position, the adjustment steps are all the same expect that the adjustment direction is opposite.

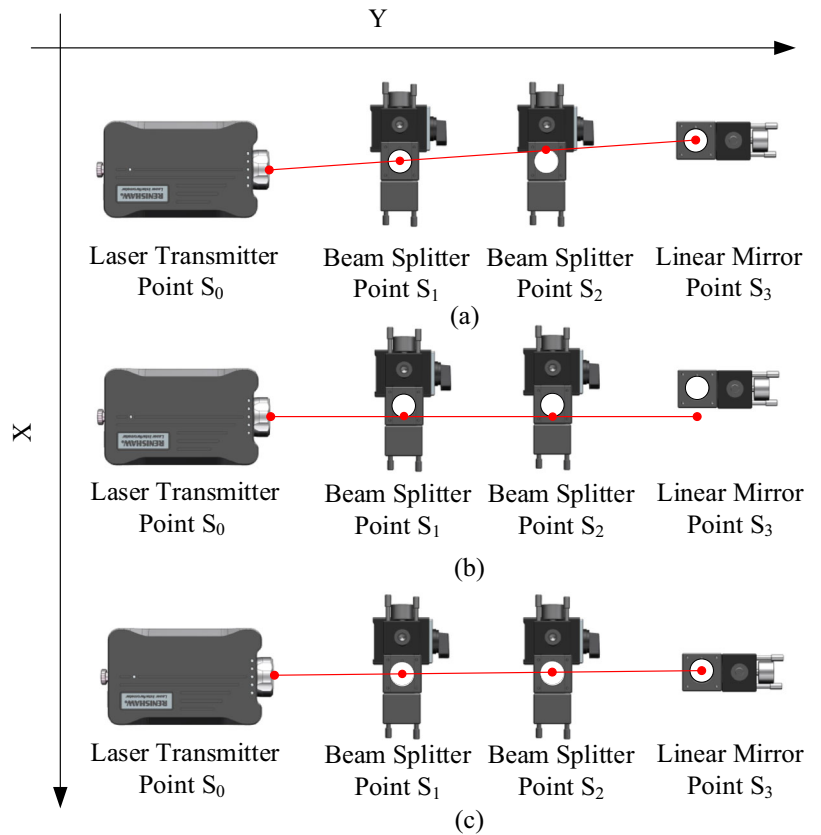
2. Adjustment of the right side optical path to the center.

Figure 22 depicts the adjustment process of the right side optical path of the Z-axis to the center. First, the laser transmitter yaw angle knob is adjusted according to the laser yaw angle  ${}^Z\varepsilon_z(l)$  to cancel it, as shown in Fig. 22b. Then, the laser transmitter is moved left based on the deviation  ${}^Z\delta_x(l)$  and the beam splitter is moved left based on the direction  ${}^Z\delta_x(s)$ ,

**Fig. 19** Adjustment of the upper optical path of the Y-axis. **a** Initial optical path. **b** Adjustment of the pitch angle error. **c** Adjustment of the translation errors



**Fig. 20** Adjustment of the right side optical path of the Y-axis. **a** Initial optical path. **b** Adjustment of the yaw angle error. **c** Adjust of the translation errors





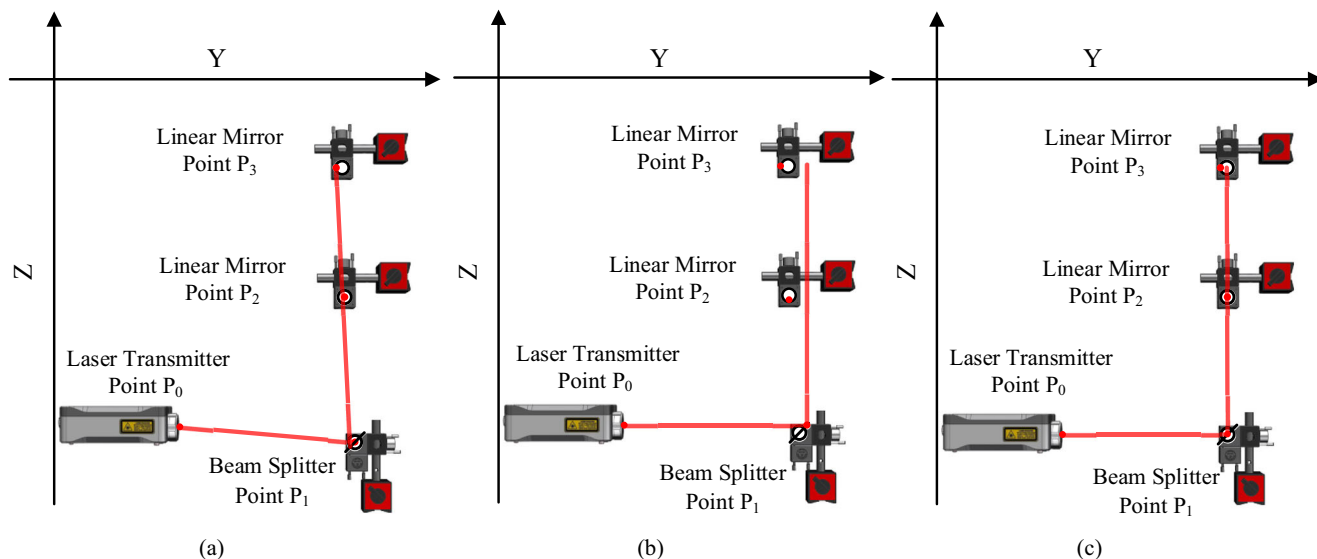


Fig. 21 Adjustment of the upper optical path of the Z-axis. a Initial optical path. b Adjustment of the pitch angle error. c Adjustment of the translation errors

respectively. Finally, the beam splitter point  $P_1$  and the linear mirror point  $P_2$  are at the center of the light target, as shown in Fig. 22c. It should be noted that when the laser transmitter  $P_0$  is located on the left side of its ideal position, the adjustment steps are all the same except that the adjustment direction is opposite.

### 6 Conclusions

A novel optical path calibration process of the linear axis of a three-axis machine tool using a Renishaw XL-80 laser interferometer is proposed in this paper. The homogeneous

coordinate transformation error model of the measured axis is established. Using the established error model, only the initial distance from the laser transmitter to the beam splitter and the initial distance from the beam splitter to the linear mirror are required to accurately calibrate the laser beam. The relationship between the fixed distance from the center of the light target to the quarter point on the edge of the light target as well as the movement distance of the measured axis are obtained. Eight deviations of the optical path affected by the laser transmitter, the beam splitter, and the linear mirror are solved. Calibrations based on the deviations can be achieved by adjusting the positions and orientations of the laser interferometer components, leading to a rapid and accurate calibration method for measuring the optical paths.

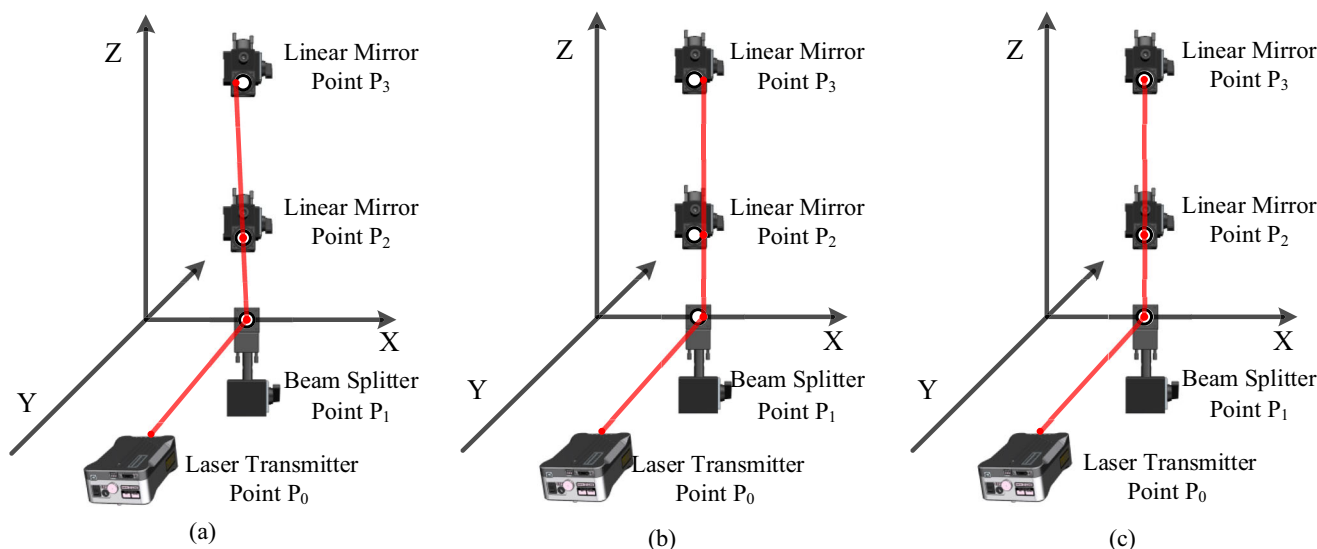


Fig. 22 Adjustment of the right side optical path of the Z-axis. a Initial optical path. b Adjustment of the yaw angle error. c Adjustment of the translation errors

**Funding** The study received financial support from the National Natural Science Foundation of China (Nos. 51905377 and 51705362) and Natural Science Foundation of Tianjin (Nos. 16JCYBJC41300 and 18JCQNJC75600).

## References

- Li J, Mei B, Shuai C, Liu XJ, Liu D (2019) A volumetric positioning error compensation method for five-axis machine tools. *Int J Adv Manuf Technol* 103:3979–3989
- Liu C, Xiang ST, Lu CW, Wu CY, Du ZC, Yang JG (2020) Dynamic and static error identification and separation method for three-axis CNC machine tools based on feature workpiece cutting. *Int J Adv Manuf Technol* 107:2227–2238
- (1994) Laser interferometer for calibrating position and accuracy. *Modern Machine Shop* 67(7):236
- Zhang M (2006) The geometric error detection and distinguishing of laser interferometer—based NC machine tool. *Mach Eng* 9:76–78
- Suo R, Fan ZJ, Li Y, Zhang SL (2004) Dual-frequency Laser Interferometer Present State and Development. *Laser Infrared* 04: 251–253
- Tipton H (1983) Use of the laser interferometer in the calibration of numerically controlled machine tools. *Opt Sens Tech Benefits Costs* 376(6):15–19
- Sun G, He G, Zhang D (2020) Body diagonal error measurement and evaluation of a multiaxis machine tool using a multibeam laser interferometer. *Int J Adv Manuf Technol* 107:4545–4559
- Peng W, Xia H, Wang S (2018) Measurement and identification of geometric errors of translational axis based on sensitivity analysis for ultra-precision machine tools. *Int J Adv Manuf Technol* 94: 2905–2917
- Li J, Xie F, Liu X (2016) Geometric error identification and compensation of linear axes based on a novel 13-line method. *Int J Adv Manuf Technol* 87:2269–2283
- Chen TR (2016) The common errors in two-frequency laser interferometry system are discussed briefly. *Shandong Ind Technol* 14: 287
- Zhuang HQ, Motaghedi SH, Roth ZS, Bai Y (2003) Calibration of multi-beam laser tracking systems. *Robot Comput Integr Manuf* 19(4):301–314
- Roux R (1995) Interferometer calibrates laser wavelengths. *Laser Focus World* 131(11):16
- Schussler H-H (1985) Comparison and calibration of laser interferometer systems. *Measurement* 3(4):175–184
- Chen GC (1992) Adjustment method of optical path of double-frequency laser interferometer in machine tool coordinate measurement. *Tool Technol* 12:40–42
- Zhang H, Zhou YF, Tang XQ (2002) Research on automatic aiming measurement and compensation technology of laser interferometer for error of CNC machine tools. *Chin J Mech Eng* 38(9):96–100
- Wei C (2007) Tips for using laser interferometer. *Metrol Meas Tech* 10:38–39
- Liu QJ, Gao HL, Wang QJ, Zheng BB (2012) Design of light collimation system for fast adjusting laser interferometer. *Mach Des Manuf* 5:59–61
- Shi JZ (2014) A fast and accurate adjustment method of laser interferometer—adjustment according to proportional method. *Manuf Technol Mach Tools* 5:99–101
- Wu SJ, Fan J, Huang ZY, Hao X (2016) The adjust laser beam practice of dual—frequency laser interferometer system measuring erect axes. *Metrol Meas Tech* 43(11):30–31
- Gong T, Liu SR (2018) Laser interferometer light path fast regulation method analysis. *Dual-use technology and products* 16: 79
- Renishaw XL-80 Laser Interferometer Operation Manual. <http://www.renishaw.com/>. Accessed 17 Feb 2020
- Barman S, Sen R (2012) Performance evaluation of multi-axis CNC machine tools by interferometry principle using laser calibration system. *J Inst Eng (India): Series C* 93(2):151–155

**Publisher's note** Springer Nature remains neutral with regard to jurisdictional claims in published maps and institutional affiliations.